Virtual Cell Based Resource Allocation for Efficient Frequency Utilization in Unmanned Aircraft Systems

Daisuke Takaishi, *Student Member, IEEE*, Yuichi Kawamoto, *Member, IEEE*, Hiroki Nishiyama, *Senior Member, IEEE*, Nei Kato, *Fellow, IEEE*, Fumie Ono, *Member, IEEE*, and Ryu Miura, *Member, IEEE*

***Abstract*—Recently, unmanned aircraft systems (UASs) have attracted attention as a new avenue for commercial services. Using the flexible mobility of unmanned aircrafts (UAs), commercial services can be operated in wide areas. However, there is a problem in the wireless communication between the UA and its ground station. When several UASs are operated within the neighboring airspace, wireless-communication conflicts occur. One of the most effective solutions for this issue is to decide the communication schedule using a time-division multiple access (TDMA) scheme. Furthermore, by spatially reusing the time slot, numerous UAs can be operated within the neighboring airspace, in a limited frequency band. In this paper, we propose an efficient time-slot allocation for enhancing the frequency resource utilization. Our proposed scheme determines the time-slot allocation considering the time-slot spatial reuse, using a virtual cell based space partitioning method. In addition, we consider the influence of the UA mobility on the network to decide the parameters for the proposed resource allocation system. The effectiveness of our proposed resource allocation is evaluated through computer-based simulation.**

***Index Terms*—Unmanned aircraft system (UAS), unmanned aircraft (UA), channel access method, time division multiple access (TDMA), virtual cell-based.**

I. Introduction

In RECENT years, unmanned aircraft systems (UASs) have become a prominent choice for commercial applications. There are several possible reasons for UAS, which were mainly used for military purposes including post-disaster damage assessments and military reconnaissance[1]–[7], to garner attention for civilian applications. The most significant among reasons is that unmanned-aircraft (UA) control has been facilitated by the advancements in control technology. This is also attributed to the fact that high-performance UAs can be purchased at affordable prices due to the advances in carbon fiber-reinforced plastic materials, energy storage, and communication. Examples of civilian UAS applications, which have elicited interest, include operation in wide areas and in places where people cannot enter (e.g., crop monitoring, geographical mapping, etc.) [8]–[13]. In these applications, data obtained from video cameras equipped on the UA are sent to the ground station, in real time. However, there are problems in the wireless communication between the UA and its ground station. In an environment, where several UASs are operated in the vicinity, video- packet drops occur, owing to interference from the other UASs. In future, the number of UAs is expected to increase drastically, while the available frequency continues to remain limited. Therefore, a frequency resource allocation system is crucial for efficiently using the limited frequency band. In this paper, we present the results of a project, under the initiative of the Ministry of Internal Affairs and Communication, in Japan, for advancing the data transmission between the UAs and the ground station, by the high- efficiency usage of the limited frequency bands.

There are several approaches for improving the frequency resource utilization, which can be adopted to UASs [14]–[18]. Spatial time division multiple access (STDMA) is a famous access scheme for improving resource utilization [19]–[23]. In this scheme, the frequency resource is divided into several time-slots and a time-slot is allocated to several transmitting nodes; i.e., several nodes are scheduled to transmit data simultaneously. Consequently, this simultaneous data transmission improves the sum of the throughput. Therefore, the resource utilization efficiency per unit area improves. In these works, the spatial time-slot allocation for several nodes is decided, based on the position coordinates of both the senders and receivers. If the distance between communication pairs, composed of a sender and receiver, is sufficiently large, a time-slot can be allocated to these pairs. However, there is the problem with the amount of calculation needed because the spatial reuse of a time-slot should be decided, based on the position coordinates of all the nodes. Additionally, there is a stability problem in the spatial reuse of time-slots [23]. As the spatial reuse of time-slots is determined by calculation, based on the current node's position coordinates, simultaneous communication cannot be performed correctly, when the nodes move and the position coordinates change.

Manuscript received June 15, 2017; revised September 21, 2017 and October 19, 2017; accepted October 22, 2017. Date of publication November 21, 2017; date of current version April 16, 2018. This paper was supported by the Ministry of Internal Affairs and Communications, Japan, under the national project, Research and Development of Communication Network Technology for Efficient Use of Frequency in Unmanned Aircraft Systems. The review of this paper was coordinated by Prof. Y. Qian. *(Corresponding author: Daisuke Takaishi.)*

D. Takaishi, Y. Kawamoto, H. Nishiyama, and N. Kato are with the Graduate School of Information Sciences, Tohoku University, Sendai 980-8577, Japan (e-mail: daisuke.takaishi@it.is.tohoku.ac.jp; youpsan@it.is.tohoku.ac.jp; hiroki.nishiyama.1983@ieee.org; kato@it.is.tohoku.ac.jp).

F. Ono and R. Miura are with the National Institute of Information and Communications Technology, Tokyo 184-8795, Japan (e-mail: fumie@nict.go.jp; ryu@nict.go.jp).

Color versions of one or more of the figures in this paper are available online at http://ieeexplore.ieee.org.

Digital Object Identifier 10.1109/TVT.2017.2776240

On the other hand, some researchers have proposed resource allocation schemes, based on the space partitioning method [24]–[27]. In these schemes, the nodes that can communicate simultaneously are decided by partitioning the network field. Within a partitioned area, only one node can communicate at a time and the TDMA scheme is used, when there are two or more nodes in the area; simultaneous communications are performed with nodes located in different partition areas. Thus, the frequency resource utilization is increased. This resource allocation scheme has a higher stability than the STDMA scheme because simultaneous communication can be performed, even when nodes move within their own partitioned area.

In previous research, the stability problem with simultaneous communication is because node mobility was not considered, when deciding the time-slot allocation. In this paper, we propose a frequency resource allocation system for UASs, with high mobility. Our proposed method is based on the space partitioning method and the field is virtually divided into several hexagonal cells (virtual cells). With calculations based on the virtual cell-based network model, the proposed method can uniquely decide the spatial reuse of time-slots for UASs. In order to enable stable simultaneous communication, the radius of the virtual cell is decided, based on the UA speed; we first focus on the length of the cycle for updating the UAS resource allocation (resource allocation cycle). We analyze the influence of the resource allocation cycle on the resource utilization efficiency and propose an optimal decision scheme for the length of the resource allocation cycle. Then, we propose a method for determining the number of time-slots allocated to each UA.

The remainder of this paper is organized as follows: The network scenario under consideration is introduced in Section II. Section III describes the proposed system model using virtual cells, based on the space partitioning method. The optimization of the parameters of the proposed system model is presented in Section IV. Section V discusses the results of the simulation, evaluating the proposed time-slot allocation scheme; the theoretical performance is also analyzed in this Section. Finally, the conclusion is provided in Section VI.

II. Communication Scenario and Supposed Network

In this section, we present an overview of the supposed network topology and communication scenario. The constraints for successful communication are also introduced.

A. Overview of the Supposed Network

As shown in Fig. 1, we assume that numerous UASs are deployed within the coverage of a resource allocation station. Each UAS is composed of a UA and a ground station. The locations of each UA and ground station are known using localization technology (i.e., global positioning systems (GPS)). For controlling the flight of the UA and monitoring the object, high-quality video data is directly transmitted from the UA to its ground station. In previous studies, each UA was assumed to use a different channel; however, the frequency band that can be used by the UAs is limited, in practice. Therefore, we assume

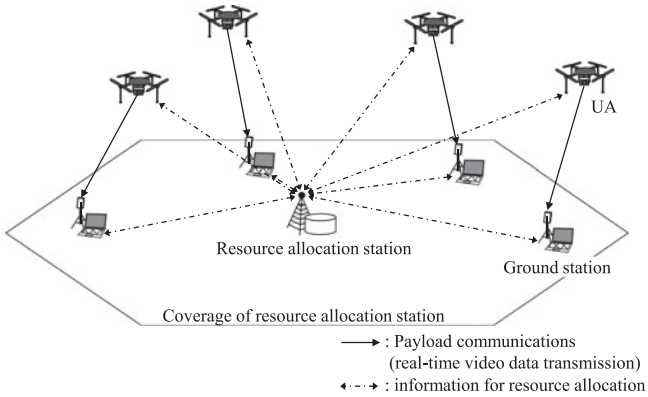

Fig. 1. Supposed network topology consisting of UASs and the resource allocation station.

that all the UA wireless transmissions use the same frequency channel.

In the case where some of the UAs share the same frequency channel, packet loss may be caused by interference from the other nodes. Therefore, we assume a TDMA-based resource allocation system. The frequency channel is divided into several time-slots and allocated to the UAs. In the supposed network, the resource allocation station decides the allocation of the time-slot for each UA. In order to decide the allocation, UA information (e.g., the position coordinates both of the UA and the ground station, the flying speed) is directly transmitted from the UASs to the resource allocation station. On the other hand, the allocation of the time-slot is informed by the resource allocation station to each UAS. These communications also use the same frequency channel as that between the UA and the ground station.

B. Communication Constraints

In this subsection, we describe the constraints for successful simultaneous communication. With respect to the constraints formulated in this subsection, we propose a cell-based resource allocation scheme, in the following sections.

If all the UAs conduct wireless transmission using different time-slots, a direct communication link between the UA and ground station can be established, if the corresponding signal-to-noise ratio (SNR) is greater than or equal to a certain threshold, γ_0, formulated as follows:

$$SNR = \frac{P_{d_u}}{N_0} \geq \gamma_0, \tag{1}$$

where, d_u is the Euclidean distance between the UA and the ground station of the UAS, u. This value is calculated using the difference between the height and horizontal distance of the UA and ground station. N_0 is the background noise power spectral density, and P_{d_u} is the received strength of the signal at the ground station of the UAS, u, expressed as follows:

$$P_{d_u} = P_{\mathrm{t}} \left(\frac{\lambda}{4\pi d_u} \right)^2 G_{\mathrm{t}} G_{\mathrm{r}}, \tag{2}$$

where P_{t} is the transmission power and λ is the wave length of the carrier band; G_{t} and G_{r} are the antenna gains of the

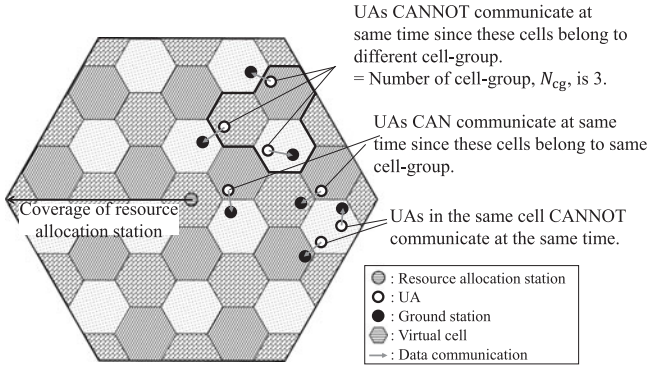

Fig. 2. Proposed virtual cell-based network structure, with three cell-groups and the communication policies.

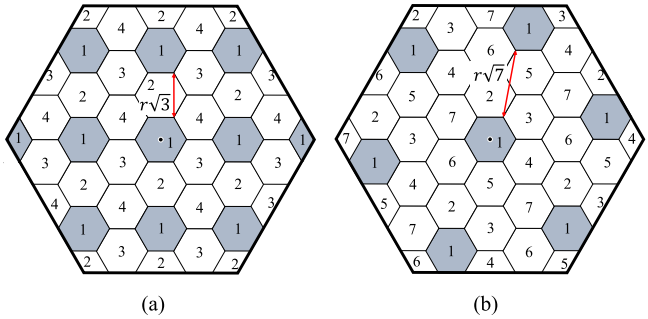

Fig. 3. Number of cell-groups and the distance between cells belonging to the same cell-group. (a) Cell-groups = 4. (b) Cell-groups = 7.

transmitter and receiver, respectively. In our research, a free-space model is used as the radio propagation model between the UAs and the ground station, and we suppose that the antenna has no directivity.

On the other hand, in the case where certain UAs simultaneously transmit data using a frequency channel, each ground station can successfully receive the data, when the signal-to-interference ratio (SIR) is greater than or equal to a certain threshold, γ_0, expressed as follows:

$$SIR = \frac{P_{d_u}}{I_u} \geq \gamma_0, \tag{3}$$

where I_u is the sum of the interference signal strength at the ground station of the UAS, u. The theoretical maximum capacity of the links can be formulated, based on the Shannon-Hartley theorem [28], as follows:

$$\theta = B \cdot \log_2 (1 + SIR), \tag{4}$$

where B is the bandwidth of the frequency channel.

III. Virtual Cell-Based Resource Allocation

In this section, we propose a virtual cell-based resource allocation method for efficient frequency utilization for UASs. In our proposed method, the spatial reuse of the time-slots is decided, based on a virtual cell-based network topology. The time-slot allocation decision scheme is also described, in this section. We describe the derivation of the optimal value of the parameters of the proposed system in following section.

A. Communication Policies for Spatial Time-Slot Reuse

Fig. 2 shows the overview of the proposed cell-based network structure. In order to decide the set of UAs that can communicate simultaneously, we use a virtual cell-based space partitioning method. In our proposed system, numerous virtual cells having the same radius, r, are located over the coverage area of the resource allocation station. Each UA and its ground station are in a virtual cell. Here, the UA and its ground station are not necessarily located in the same virtual cell. The resource allocation for each UAS is decided such that packet drops, caused by interference from the other UAs, do not occur, even if the UA distribution is not uniform. Hence, the time-slot allocation and radius of the virtual cell should be decided, when the SIRs of all the UASs satisfy the requirement depicted in (3). Additionally, to enhance the frequency utilization, it is necessary to increase the number of UAs that spatially reuse the time-slots. Therefore, our proposed system adopts a fractal virtual cell placement, which can improve the number of UAs that can communicate simultaneously. Fig. 2 is an example of virtual-cell placement, when the number of "cell-groups" is three. In Fig. 2, the fill pattern of the cells indicates that they belong to the same "cell-group". In this paper, a "cell-group" is a set of cells in which the UAs can transmit data simultaneously. UAs cannot transmit data simultaneously with other UAs that are in a cell belonging to a different cell-group. This is because the SIR requirement cannot be satisfied, when a UA transmits data using the same time-slot as that used by other UAs belonging to different cell-groups; depending upon the positions of the UAs and the ground station, it may be satisfied but not always. Similarly, to always satisfy the SIR requirement, only one UA can communicate at a time, in each cell. Fig. 3 displays examples in which the number of cell-groups are four and seven, respectively. In Fig. 3, the number written in each cell identifies the cell-group. Generally, the value of the cell-group is determined based on the performance of wireless modules, such as the required length of the guard-time between time-slots. Therefore, we suppose the number of the cell-group as the given value. The effect of the number of the cell-group is evaluated in the following section.

B. Time-Slot Allocation

As mentioned in the previous section, we assume a TDMA-based resource allocation and that the frequency channel is divided into several time-slots. Fig. 4 depicts the proposed communication frame structure. We propose a superframe-based frame structure. Each superframe consists of control and payload frames, i.e., the sum of the lengths of the control and payload frames is equal to the length of the superframe. During the control frames, the time-slot allocations are informed by the resource allocation station to the UASs. In addition, the UAS information (e.g., the current position coordinates and flying speed of the UAs) from the UASs to the resource allocation station is aggregated for deciding the time-slot allocation. On the other hand, during a payload frame, each UA is scheduled

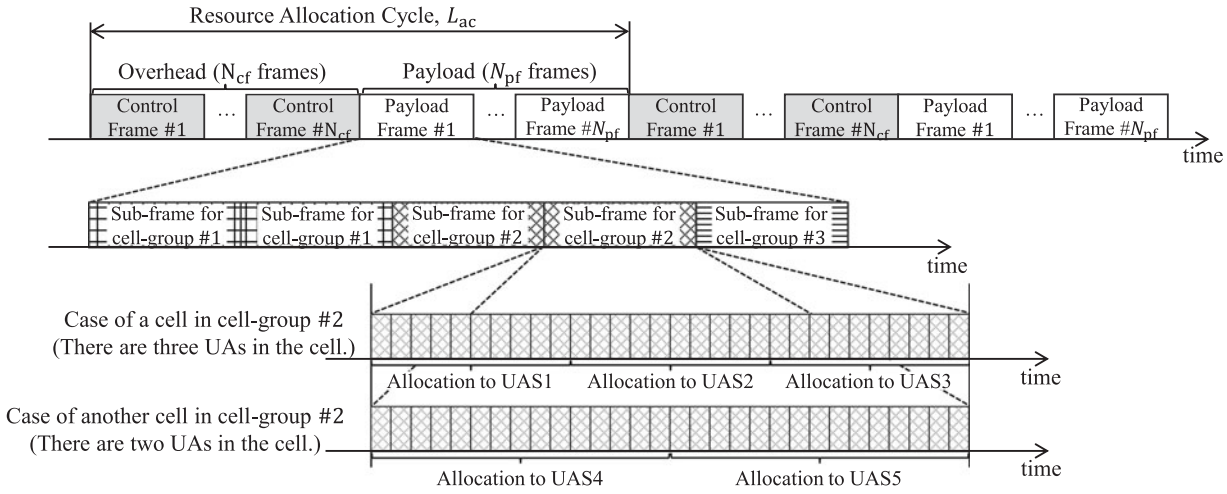

Fig. 4. Proposed time-slot structure.

to transmit data (e.g., real-time video data packets and observed environmental information) once. The length of the transmission from each UA in each superframe differs, depending upon the number of allocated time-slots. However, if the length of the superframe, $L_{\rm ac}$, is considerable, the interval from one transmission to the next, for each UA, increases. Therefore, we assume that each superframe, consisting of certain payload frames, decreases such communication delays.

As mentioned earlier, in order to always satisfy the SIR requirement in (3), UAs in cells belonging to different cell-groups cannot communicate simultaneously. Therefore, each payload frame is divided into subframes, equal to the number of cell-groups, $N_{\rm cg}$. Moreover, to always satisfy the SIR requirement, only one UA can communicate in a cell, and the subframes are divided into time-slots and evenly allocated to the UAs. Fig. 4 shows an example of the case, where there are two or three UAs in the cell, c, belonging to the 2nd cell-group.

In the proposed system, the resource allocation station calculates the virtual cell information (i.e., the number of UAs located in each virtual cell, and the distance between the UA and its ground station), based on the aggregated information from each UAS. Then, the time-slot allocation is determined using this cell information. As the network environment changes owing to UA movements, the UAS information is collected periodically and the time-slot allocation is updated. However, as the calculation for the allocation starts only after collecting the information from all the UASs, it is impossible to notify the allocation in the same superframe. Thus, the allocation notification is sent in the control frame of the next superframe. This is a common feature of the TDMA scheme. In the following section, we describe the problem caused by this feature and propose a decision scheme for the resource allocation cycle, to address this problem.

IV. Derivation of the Optimal Values of the Parameters for the Proposed Resource Allocation System

For enhancing the frequency utilization, while satisfying the SIR requirement, the parameters in our proposed resource allocation method are to be suitably determined. In this section, we describe the problem and the parameter decision scheme.

A. Objective of the Parameter Decision Scheme

In the proposed system, at first, the radius of the virtual cell and the length of the resource allocation cycle are decided using information aggregated during the control frames. Then, the virtual cells are applied over the network. Next, the proposed system calculates the time-slot allocation using the number of UAs in each cell. In this section, we describe the parameter decision schemes for the proposed system model in order to enhance the frequency utilization. The objective of this parameter decision scheme is to maximize the frequency utilization, while all the UASs satisfy the SIR requirement. Our proposed system has three procedures: deciding the radius of the virtual cells, deciding the optimal resource-allocation cycle, and deciding the optimal time-slot allocation. In this subsection, we discuss these parameter decisions. First, we focus on the radius of the virtual cell, r. The size of the virtual cell affects parameters such as the number of UAs that can communicate simultaneously and the interference strength from the other cells. From these relationships, we derive the optimal radius of the virtual cell. Next, we describe the effect of the length of the resource allocation cycle, $L_{\rm ac}$. The frame efficiency, which is the ratio of the payload frame to the superframe, is a parameter that varies with $L_{\rm ac}$; the sum of the throughput of the UASs also varies with $L_{\rm ac}$. Hence, we analyze these relationships and derive the optimal values of $L_{\rm ac}$. Finally, we specify the UA distribution problem; differences in the throughput of the UAS are caused by the UA distribution. In order to solve this problem, we propose an optimal time-slot allocation scheme for each UAS.

By calculating these parameters in each superframe, our proposed scheme improves the frequency utilization. The parameters used in this paper are listed in Table I.

B. Radius of the Virtual Cell

The radius of the virtual cell is decided considering the UA mobility. The objective of the decision regarding the radius is

TABLE I
PARAMETER DEFINITION

Notation	Description
L_{ac}	Length of the resource allocation cycle
L_{f}	Lengths of the control and payload frames
$L_{\mathrm{sf,g}}$	Length of a subframe in a payload frame allocated to the cell-group, g
N_{cf}	Number of control frames within a resource allocation cycle
N_{pf}	Number of payload frames within a resource allocation cycle
d_u	Physical distance between the UA and the ground station of the UAS u.
$\mathcal{U}$	Set of all UASs
$\mathcal{C}$	Set of all the virtual cells
$\mathcal{C}_g$	Set of virtual cells that belong to the cell-group, g
$\mathcal{G}$	Set of all cell-groups
V_c	Number of UAs in the virtual cell, c
r	Radius of the virtual cell
β	Coefficient of the virtual-cell radius that varies according to the number of cell-groups
γ_0	SIR threshold.
N_{cg}	Number of cell-groups
A_{ras}	Coverage of the resource allocation station
B	Frequency bandwidth
P_{t}	UA transmission power
G_{t}	Antenna gain of the transmitter
G_{r}	Antenna gain of the receiver
N_0	Background noise power spectral density
P_d	Received signal strength transmitted from a distant, d
I_u	Sum of the noise strengths of the neighboring cells using the same time-slot at the ground station of the UAS, u
v	Maximum flying speed of the UAs
$G_{\mathrm{t}}, G_{\mathrm{r}}$	Antenna gain of the transmitter and receiver, respectively

to construct a communication environment in which the SIR is always larger than or equal to a certain value, regardless of where the UASs are located. Additionally, in an actual scenario, the UASs are not always distributed uniformly, and the distance between a UA and its ground station differs from that of the other UASs. Therefore, the radius of the virtual cell should be decided such that it is effective, even in this scenario.

First, we describe the method for determining the radius of the virtual cell in an environment, where the UAs are stationery, for understanding purposes. In order to satisfy the SIR requirement, it is necessary to determine the radius of the virtual cell, considering the interference strength. In our proposed system, interference indicates the data transmitted by the UASs in other virtual cells belonging to the same cell-group. By satisfying the SIR requirement even in an environment, where the SIR is the lowest in the network, all the UASs can always satisfy the requirement. Then, a spatial time-slot can be available, when the UA distribution is not uniform. According to (3), if d_u is fixed, the SIR is the lowest, when the interference is maximum. Therefore, the SIR is the lowest, when the distance between the ground-station and the interference UA is the least. Fig. 5 shows the deployment of the UA, the ground station, and the interference UA, when the SIR value is the least, if the number of cell-groups is three. When the number of cell-groups is three, the shortest distance between the cells belonging to the same cell-group is r. Therefore, the shortest distance between the interference UA and the ground station is $r - d_u$, where d_u is the distance between the UA and the ground station of the UAS, u. Although interference also occurs from other UAs in cells belonging to the same cell-group, the interference strength is considerably lesser than the maximum. Therefore, they can be neglected. We use the longest d_u among the UASs to minimize the SIR value, as follows:

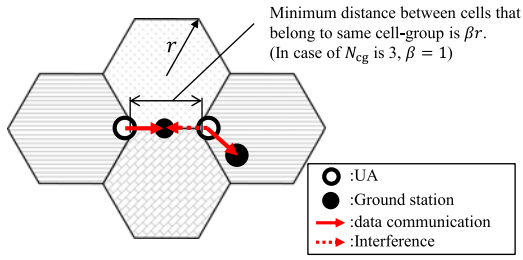

Fig. 5. Interference from the other UAs in cells belonging to the same cell-group, if the number of cell-groups is three.

$$d_{\max} = \max_{u \in \mathcal{U}} d_u, \tag{5}$$

where $\mathcal{U}$ is the set of all UASs. From (2), (3) and (5), the radius of the virtual cell is formulated as follows:

$$\frac{P_{d_{\max}}}{P_{r-d_{\max}}} \geq \gamma_0 \tag{6}$$

$$\beta r \geq d_{\max} + d_{\max}\sqrt{\gamma_0}, \tag{7}$$

where r is the radius of the virtual cell and β is the coefficient of the radius, which changes according to the number of cell-groups. When the number of cell-groups are three, four, and seven, β is 1, $\sqrt{3}$, and $\sqrt{7}$, respectively. Let $\beta r = d_{\max} + d_{\max}\sqrt{\gamma_0}$, as a smaller virtual cell radius improves the frequency utilization, as mentioned later. With this virtual cell radius calculation, all the UASs can always satisfy the SIR requirements, when the UAs are not moving.

Using the stationary environment equation, we formulate the radius of the virtual cell in an environment, where the UAs are moving. As mentioned in the previous subsection, the assignments of the resource, calculated based on the UAS information, are reflected in the next superframe. Therefore, to always satisfy the SIR requirement, all the UAs are required to remain in the current cell, even during the next superframe. Here, let v be the maximum speed of the UAs. Then, the maximum value of the movable distance, until the end of next superframe, is calculated as $2 \cdot v \cdot L_{\mathrm{ac}}$. Because the maximum allowable value for the distance between the UA and ground station is $d_{\max} + 2 \cdot v \cdot L_{\mathrm{ac}}$, until the end of next superframe, the radius of the virtual cell is decided using this value, as follows:

$$\beta r = \left(d_{\max} + 2vL_{\mathrm{ac}}\right)\left(1 + \sqrt{\gamma_0}\right). \tag{8}$$

By thus determining the virtual cell radius, the proposed method always ensures that the requirement is satisfied, even if the UAs are moving.

C. Optimal Length of the Resource Allocation Cycle

From (8), it is understood that the radius of the virtual cell increases in proportion with the resource allocation cycle, $L_{\rm ac}$. Therefore, more virtual cells can be located over the coverage of the resource allocation station, when the length of the resource allocation cycle, $L_{\rm ac}$ is less. Then, the sum of the throughput of the UASs can be increased because the number of UAs using the same time-slot increases. The sum of the throughput in a network in which there is one UA in each cell is formulated as follows:

$$\theta_{\rm sum} = B \cdot \log_2 (1+\gamma_0) \cdot \frac{N_{\rm vc}}{N_{\rm cg}}, \tag{9}$$

where $N_{\rm vc}$ is the number of virtual cells located over the coverage of the resource allocation station. Here, we use γ_0 as the SIR value for evaluating the worst throughput among the UASs, when using the proposed resource allocation system; $N_{\rm vc}/N_{\rm cg}$ indicates the number of cells in which the UAs can reuse the timeslots. The number of virtual cells, $N_{\rm vc}$, is obtained as follows:

$$N_{\rm vc} = \frac{A_{\rm ras}}{A_{\rm vc}} = \frac{2A_{\rm ras}}{3\beta^2 r^2 \sqrt{3}} \tag{10}$$

$$= \frac{2A_{\rm ras}}{3\sqrt{3}\left(d_{\max}+2vL_{\rm ac}\right)^2\left(1+\sqrt{\gamma_0}\right)^2}, \tag{11}$$

where $A_{\rm ras}$ is the coverage area of the resource allocation station and $A_{\rm vc}$, the coverage area of the virtual cells. The number of virtual cells, $N_{\rm vc}$, is an integer value; however, in this paper, we treat the number of virtual cells as a real number to eliminate the effect of the network edge problem.

On the other hand, the length of the resource allocation cycle also affects the frame efficiency, which is the ratio of the length of the payload frame to the superframe. We assume that the length of the control frame is fixed, in each superframe. Then, the frame efficiency is given by,

$$\alpha = \frac{L_{\rm f} N_{\rm pf}}{L_{\rm ac}} = 1 - \frac{L_{\rm f} \cdot N_{\rm cf}}{L_{\rm ac}}, \tag{12}$$

where $N_{\rm pf}$ and $N_{\rm cf}$ are the number of payload and control frames in a superframe, and $L_{\rm f}$ is the length of each frame. From (12), it is understood that a smaller value of $L_{\rm ac}$ results in a decrease in the frame efficiency.

According to (9) and (12), there is a trade-off relationship between the sum of the throughput and the frame efficiency. If $L_{\rm ac}$ is short, the sum of the throughput increases but the frame efficiency decreases, whereas, if $L_{\rm ac}$ is long, the sum of the throughput decreases but the frame efficiency increases. We derive the optimal length of the resource allocation cycle from these factors. First, we formulate the sum of the payload data throughput using (9) and (12), as follows:

$$\theta_{\rm p} = B\log_2(1+\gamma_0) \cdot \frac{(L_{\rm ac}-L_{\rm f}N_{\rm cf})}{L_{\rm ac}} \cdot \frac{2A_{\rm ras}}{3N_{\rm cg}\sqrt{3}\left(d_{\max}+2vL_{\rm ac}\right)^2\left(1+\sqrt{\gamma_0}\right)^2}, \tag{13}$$

Calculating $\partial\theta_{\rm p}/\partial L_{\rm ac} = 0$, the optimal length of the resource allocation cycle is,

$$\frac{\partial\theta_{\rm p}}{\partial L_{\rm ac}} = B\log_2(1+\gamma_0) \cdot \frac{2A_{\rm ras}}{3N_{\rm cg}\left(1+\sqrt{\gamma_0}\right)^2\sqrt{3}} \cdot \frac{-2v^2L_{\rm ac}^2 + 3vL_{\rm f}N_{\rm c}L_{\rm ac} + d_{\max}L_{\rm f}N_{\rm c}}{\left(d_{\max}+vL_{\rm ac}\right)^2 L_{\rm ac}} \tag{14}$$

$$L_{\rm ac}^{\rm opt} = \frac{6vL_{\rm f}N_{\rm cf} + \sqrt{4vL_{\rm f}N_{\rm cf}\left(9vL_{\rm f}N_{\rm cf}+4d_{\max}\right)}}{8v}. \tag{15}$$

D. Optimal UAS Time-Slot Allocation

In this subsection, we propose a time-slot allocation scheme. To enhance the throughput, while maintaining a high fairness, our proposed scheme aims to maximize the minimum throughput among all the UAs.

Before proposing the time-slot allocation scheme, we fist describe the definition of the time-slots and subframes, and formulate the throughput of each UAS. The proposed superframe consists of control and payload frames. Further, the payload frames are divided into a number, $N_{\rm cg}$, of subframes. Therefore, the length of the payload frame always satisfies the following equation:

$$N_{\rm pf} \cdot (\Sigma_{g\in G} L_{{\rm sf,g}}) + N_{\rm cf} \cdot L_{\rm f} = L_{\rm ac}. \tag{16}$$

In order to allocate time-slots to each UA, the subframe of the cell-group to which the cell belongs is divided into time-slots. Hence, when there is only one UA in a cell, the subframes are divided into times slots and all the divided time-slots are allocated to the UA. However, if there are two or more UAs, the time-slots are equally allocated to these UAs. The sum of the time-slots allocated to one UA in a cell, c, of the cell-group, g, is formulated as follows:

$$N_{{\rm ts},c} = N_{\rm pf} \cdot L_{\rm sf,g}/V_{\rm c}. \tag{17}$$

Here, we treat the number of time-slots as a real number for simplifying the calculation. From (4), the throughput of the UA located in cell, c, is obtained as,

$$\theta_c = B \cdot \log_2(1+\gamma_0) \cdot \frac{N_{\rm pf} \cdot L_{\rm sf,g}}{V_c \cdot L_{\rm ac}}. \tag{18}$$

Next, we describe the time-slot-allocation decision scheme using virtual cells. From (18), it is obvious that the time-slot is determined by deciding the length of the subframe of each cell-group. Therefore, our resource allocation objective is to decide the lengths of the subframes for maximizing the minimum throughput among the UAs in the network. The objective function is formulated as follows:

$$L_{{\rm sf},g}^{\rm opt} = \underset{L_{\rm sf,g}}{\rm argmax}\left(\min\{\theta_{\rm c}|{\rm c}\in\mathcal{C}\}\right) = \underset{L_{\rm sf,g}}{\rm argmax}\left(B\log_2(1+\gamma_0)\frac{N_{\rm pf}L_{\rm sf,g}}{\max_{c\in\mathcal{C}_g}V_c}\cdot\frac{1}{L_{\rm ac}}\right) \tag{19}$$

where $L_{{\rm sf},g}^{\rm opt}$ is the optimal length of the subframe for the cell-group, g. The term, $\max_{c\in\mathcal{C}_g} V_c$, is the maximum value of V_c in the cell-group, g. This formula indicates that the candidates for

TABLE II
EVALUATION-PARAMETER SETTINGS

Parameter	Value
Number of UAs	100-500
Radius of the resource allocation station	5000 m
Frequency	5.7 GHz
Bandwidth	20 MHz
Transmission power	0.2 W
Background noise power spectral density (N_0)	1.0×10^{-12} W
Transmitter antenna gain	0 dBi
Receiver antenna gain	0 dBi
Number of cell-groups	3,4,7
Radio propagation model	Free space

the minimum throughput are the cells with a maximum value of V_c, among the same cell-group.

According to (16) and (19), the set of optimal subframe lengths is

$$L_{\mathrm{sf},g}^{\mathrm{opt}} = \frac{\max_{c \in \mathcal{C}_g} V_c}{\sum_{g' \in \mathcal{G}} \left(\max_{c \in \mathcal{C}_{g'}} V_c \right)}, \tag{20}$$

where, $\mathcal{G}$ is the set of all of cell-groups. Then, the number of time-slots allocated to each UA, shown in (17), is decided.

V. PERFORMANCE EVALUATION

We evaluate the performance by computer-based simulation. In this section, we first evaluate our proposal by comparison with the TDMA scheme, which evenly allocates time-slots to the UAs without considering the spatial reuse of the time-slots. Then, we evaluate our proposed method of optimizing the length of the resource allocation cycle. The effect of the UAS distribution on our proposal is also analyzed, in this section

A. Parameter Settings

Table II lists the considered parameters for our simulation scenario. Numerous UASs are deployed within the coverage of the resource allocation station. The coverage area radius of the resource allocation station is set to 5000 m. All the UAs transmit data using the time-slot allocated by the resource allocation station. The performances of the communication modules used in all the UASs are assumed to be the same. The frequency and bandwidth are set, based on the actual values available for UASs in Japan. A free-space radio propagation model is used between the UA and its ground station. In the proposed resource allocation system, the number of cell-groups is set to three, four, and seven, respectively. The time-slot allocation is decided by (20), in the proposed resource allocation.

B. Comparison With Traditional TDMA

In this experiment, we evaluate the frequency utilization by comparing the throughput with the TDMA scheme. In the TDMA scheme, time-slots are evenly allocated to all the UAs. In this simulation, the UAS distribution is set to be uniform. To evaluate the performance, based on the worst SIR value, we set the distances between all the UAs and ground stations to 400 m. The simulation result is demonstrated in Fig. 6, in terms of the minimum throughput among all the UAs. The plot in the figure shows that for the TDMA scheme, the throughput gradually decreases with the increase in the number of UAs. The same trend can be observed for our proposed resource allocation. However, our proposal exhibits a considerably higher throughput. This difference is based on whether the resource allocation scheme calculation considers the spatially reuse of the time-slots.

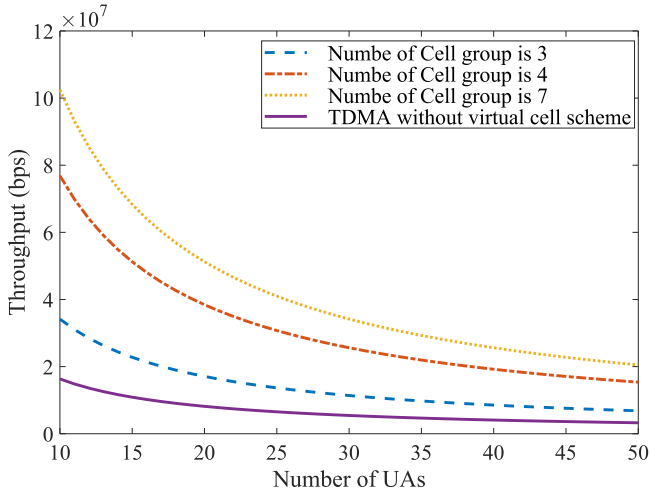

Fig. 6. Frequency utilization.

C. Optimal Length of the Allocation Cycle

To evaluate our proposed method for optimizing the length of the resource allocation cycle, we measure the sum of the throughput among the distributed UASs by varying the length of the resource allocation cycle. We set the sum of the control frame lengths to 10 ms, in each resource allocation cycle; the maximum speed of the UAs is set to 5 m/s, 10 m/s, and 20 m/s, respectively.

Fig. 7(a) depicts the trade-off relationship between the sum of the throughput and the frame efficiency. Fig. 7(b) depicts the sum of the payload data throughput and the optimal resource allocation cycle. The black dots indicate the optimal length of the resource allocation cycle computed using our method. With our method, the optimal length of the resource allocation cycle is determined to be 2.7 s, 2.0 s, and 1.6 s, when the maximum UA speed is 5 m/s, 10 m/s, and 20 m/s, respectively. These results show that our method can decide the optimal length of the resource allocation cycle for maximizing the sum of the payload throughput of the distributed UASs.

D. Theoretical Throughput

Next, we analyze the lower and upper bounds of the minimum throughput among the UASs, when our proposed time-slot allocation scheme is used. From (19), it can be observed that our proposed time-slot allocation is calculated, using the maximum number of UAs in each cell-group. This is because the cell with

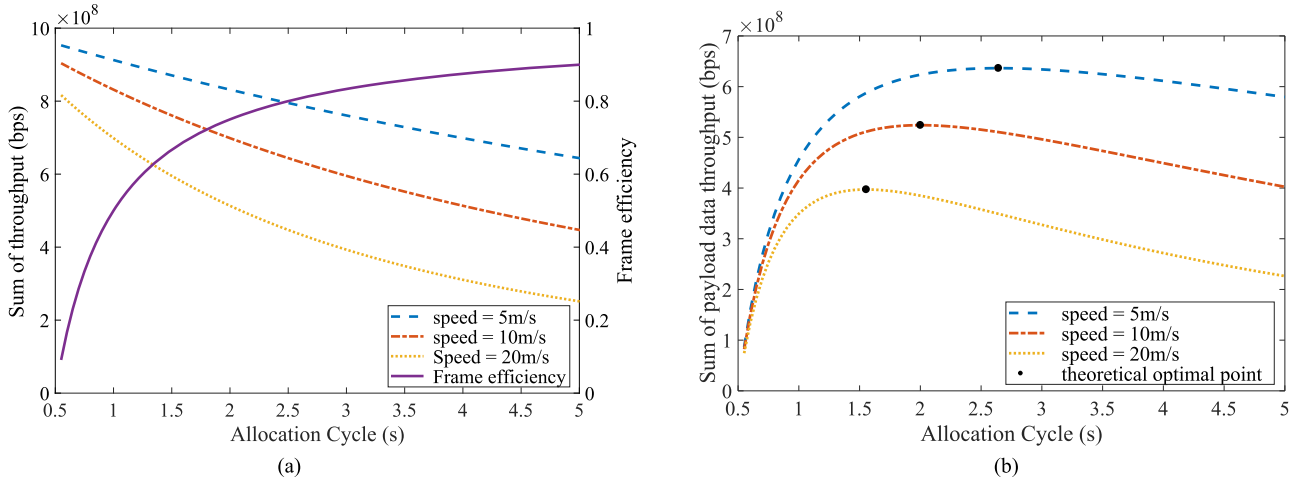

Fig. 7. Effect of the length of the resource allocation cycle. (a) Effect of the resource allocation cycle on the sum of the throughput and frame efficiency. (b) Sum of the payload data throughput and optimal resource allocation cycle.

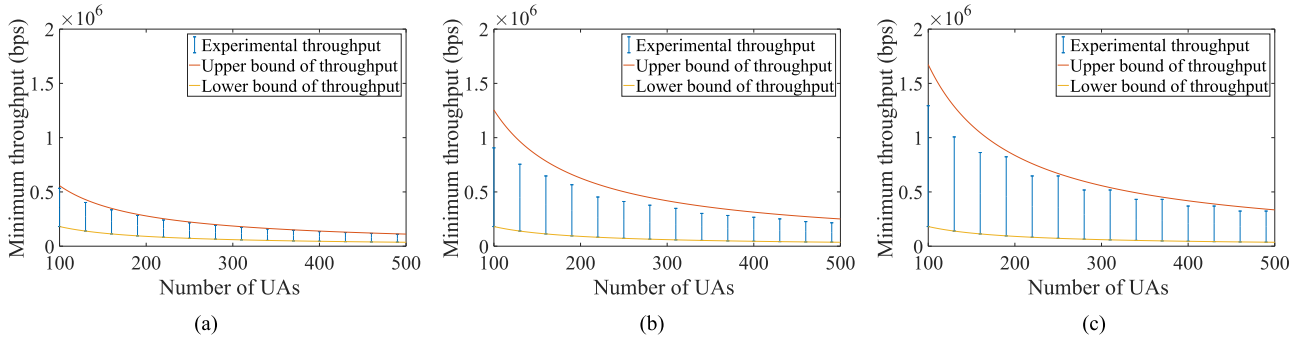

Fig. 8. Effect of UA distribution. (a) Number of cell-group is 3. (b) Number of cell-group is 4. (c) Number of cell-group is 7.

the largest number of UAs in each cell-group can be a candidate for the minimum throughput. In addition, the minimum values of the throughput of all the cell-groups are determined to be equal. Then, the minimum throughput among the UASs is formulated as follows:

$$\min\left\{\theta_c \middle|\, \forall c \in \mathcal{C}\right\} = \frac{\alpha B \log_2\left(1+\gamma_0\right)}{\sum_{g\in\mathcal{G}} \max\left\{\mathrm{V}_{c'} \middle|\, \forall \mathrm{c}' \in \mathcal{C}_{\mathrm{g}}\right\}}. \tag{21}$$

First, we consider the UA deployment that minimizes (21). To minimize (21), the denominator is maximized. This is the case, where all the UAs are located in one cell of each cell-group. Therefore, the denominator of the equation is $|\mathcal{U}|$. Then, the lower bound of the minimum throughput is

$$\theta^{\mathrm{lower}} = \frac{\alpha}{|\mathcal{U}|} B \log_2\left(1+\gamma_0\right). \tag{22}$$

Next, we consider the UA deployment that maximizes (21). To maximize (21), the denominator is minimized. This is the case, where all the UAs are evenly located in all the cells. Therefore, the denominator of the equation is $\frac{|U|}{N_{\mathrm{vc}}} \cdot N_{\mathrm{cg}}$. Thus, the upper bound of the minimum throughput is

$$\theta^{\mathrm{upper}} = \frac{\alpha \cdot N_{\mathrm{vc}}}{N_{\mathrm{cg}} \cdot |\mathcal{U}|} \cdot B \cdot \log_2\left(1+\gamma_0\right). \tag{23}$$

Next, we evaluate the effect of the UAS distribution using computer-based simulation and analyze the theoretical formulation. We measure the minimum throughput among the distributed UASs by varying the UAS distribution and the number of nodes. The UAS distributions are randomly decided, in each experiment. We conduct the simulation 100,000 times for each parameter setting. We set the distances between all the UAs and their ground stations to 700 m.

Fig. 8 shows the minimum throughput among the UASs, when the number of cell-groups are three, four, and seven, respectively. Here, the error bar indicates the minimum throughput range measured in the experiment; the theoretical upper and lower bounds are also depicted, in these figures. From these results, it can be confirmed that the lower and upper bounds formulated in this paper agree with the experimental values.

VI. Conclusion

In this paper, we have presented a resource allocation system for data transmission from a UA to a ground station. In order to select UAs that can communicate simultaneously, the proposed resource allocation system uses a space partitioning method in which the target field is divided into virtual hexagonal cells. First, we have proposed a decision scheme for the virtual cell radius. By calculating the radius, based on the resource allocation cycle and the UA flying speed, the proposed method can achieve high frequency utilization, even when UA movement occurs. Furthermore, we have indicated the problem of the variation in the number of UAs in each virtual cell; a time-slot allocation for each UA that maximizes the throughput was proposed. The upper and lower bounds of this proposed resource allocation system were also formulated. Numerical results were presented to verify the effectiveness of our proposal.

References

[1] H. Nishiyama, T. Ngo, S. Oiyama and N. Kato, "Relay by smart device: Innovative communications for efficient information sharing among vehicles and pedestrians," *IEEE Veh. Technol. Mag.*, vol. 10, no. 4, pp. 54–62, Dec. 2015.

[2] A. E. A. A. Abdulla, Z. M. Fadlullah, H. Nishiyama, N. Kato, F. Ono, and R. Miura, "Toward fair maximization of energy efficiency in multiple UAS-Aided networks: A game-theoretic methodology," *IEEE Trans. Wireless Commun.*, vol. 14, no. 1, pp. 305–316, Jan. 2015.

[3] A. E. A. A. Abdulla, Z. M. Fadlullah, H. Nishiyama, N. Kato, F. Ono, and R. Miura, "An optimal data collection technique for improved utility in UAS-aided networks," in *Proc. 33rd Annu. IEEE Int. Conf. Comput. Commun.*, Toronto, ON, Canada, May, 2014, pp. 736–744.

[4] Z. M. Fadlullah, D. Takaishi, H. Nishiyama, N. Kato, and R. Miura, "A dynamic trajectory control algorithm for improving the communication throughput and delay in UAV-aided networks," *IEEE Netw. Mag.*, vol. 30, no. 1, pp. 100–105, Jan. 2016.

[5] F. Ono, H. Ochiai, and R. Miura, "A wireless relay network based on unmanned aircraft system with rate optimization," *IEEE Trans. Wireless Commun.*, vol. 15, no. 11, pp. 7699–7708, Nov. 2016.

[6] Y. Zeng, R. Zhang, and T. J. Lim, "Wireless communications with unmanned aerial vehicles: opportunities and challenges," *IEEE Commun. Mag.*, vol. 54, no. 5, pp. 36–42, May 2016.

[7] M. Mozaffari, W. Saad, M. Bennis and M. Debbah, "Efficient deployment of multiple unmanned aerial vehicles for optimal wireless coverage," *IEEE Commun. Lett.*, vol. 20, no. 8, pp. 1647–1650, Aug. 2016.

[8] M. Tortonesi, C. Stefanelli, E. Benvegnu, K. Ford, N. Suri, and M. Linderman, "Multiple-UAV coordination and communications in tactical edge networks," *IEEE Commun. Mag.*, vol. 50, no. 10, pp. 48–55, Oct. 2012.

[9] D. Takaishi, H. Nishiyama, N. Kato, and R. Miura, "Toward energy efficient big data gathering in densely distributed sensor networks," *IEEE Trans. Emerg. Topics Comput.*, vol. 2, no. 3, pp. 388–397, Sep. 2014.

[10] L. Gupta, R. Jain, and G. Vaszkun, "Survey of important issues in UAV communication networks," *IEEE Commun. Surveys Tuts.*, vol. 18, no. 2, pp. 1123–1152, Apr.–Jun. 2016.

[11] U. Zengin and A. Dogan, "Real-Time target tracking for autonomous UAVs in adversarial environments: A gradient search algorithm," *IEEE Trans. Robot.*, vol. 23, no. 2, pp. 294–307, Apr. 2007.

[12] H. Kwon, J. Yoder, S. Baek, S. Gruber, and D. Pack, "Maximizing target detection under sunlight reflection on water surfaces with an autonomous unmanned aerial vehicle," in *Proc. 2013 Int. Conf. Unmanned Aircr. Syst.*, Atlanta, GA, USA, Jul. 2013, pp. 17–24.

[13] M. Mozaffari, W. Saad, M. Bennis, and M. Debbah, "Unmanned aerial vehicle with underlaid device-to-device communications: Performance and tradeoffs," *IEEE Trans. Wireless Commun.*, vol. 15, no. 6, pp. 3949–3963, Jun. 2016.

[14] X. Cheng, L. Yang, and X. Shen, "D2D for intelligent transportation systems: A feasibility study," *IEEE Trans. Intell. Transp. Syst.*, vol. 16, no. 4, pp. 1784–1793, Aug. 2015.

[15] H. Zhang, C. Jiang, X. Mao, and H. H. Chen, "Interference-Limited resource optimization in cognitive femtocells with fairness and imperfect spectrum sensing," *IEEE Trans. Veh. Technol.*, vol. 65, no. 3, pp. 1761–1771, Mar. 2016.

[16] M. Peng, K. Zhang, J. Jiang, J. Wang, and W. Wang, "Energy-efficient resource assignment and power allocation in heterogeneous cloud radio access networks," *IEEE Trans. Veh. Technol.*, vol. 64, no. 11, pp. 5275–5287, Nov. 2015.

[17] J. Xu and R. Zhang, "CoMP meets smart grid: A new communication and energy cooperation paradigm," *IEEE Trans. Veh. Technol.*, vol. 64, no. 6, pp. 2476–2488, Jun. 2015.

[18] W. Zhao, H. Nishiyama, Z. M. Fadlullah, N. Kato, and K. Hamaguchi, "DAPA: Capacity optimization in wireless networks through a combined design of density of access points and partially overlapped channel allocation," *IEEE Trans. Veh. Technol.*, vol. 65, no. 5, pp. 3715–3722, May 2015.

[19] R. Nelson and L. Kleinrock, "Spatial TDMA: A collision-free multihop channel access protocol," *IEEE Trans. Commun.*, vol. 33, no. 9, pp. 934–944, Sep. 1985.

[20] K. Jain, J. Padhye, V. Padmanabhan and L. Qiu, "Impact of interference on multi-hop wireless network performance," *Proc. ACM Mobicom*, 2003, pp. 66–80.

[21] P. Phunchongharn and E. Hossain, "Distributed robust scheduling and power control for cognitive spatial-reuse TDMA networks," *IEEE J. Sel. Areas Commun.*, vol. 30, no. 10, pp. 1934–1946, Nov. 2012.

[22] P. Bjorklund, P. Varbrand, and Di Yuan, "Resource optimization of spatial TDMA in ad hoc radio networks: A column generation approach," in *Proc. 23rd Annu. IEEE Int. Conf. Comput. Commun.*, San Francisco, CA, USA, Jul. 2003, vol. 2, pp. 818–824.

[23] K. Papadaki and V. Friderikos, "Robust scheduling in spatial reuse TDMA wireless networks," *IEEE Trans. Wireless Commun.*, vol. 7, no. 12, pp. 4767–4771, Dec. 2008.

[24] P. Mitran, H. Ochiai and V. Tarokh, "Space-Time diversity enhancements using collaborative communications," *IEEE Trans. Inf. Theory*, vol. 51, no. 6, pp. 2041–2057, Jun. 2005.

[25] A. Sgora and D. D. Vergados, "Handoff prioritization and decision schemes in wireless cellular networks: A survey," *IEEE Commun. Surveys Tuts.*, vol. 11, no. 4, pp. 57–77, Oct.–Dec. 2009.

[26] L Budzisz *et al.*, "Dynamic resource provisioning for energy efficiency in wireless access networks: A survey and an outlook," *IEEE Commun. Surveys Tuts.*, vol. 16, no. 4, pp. 2259–2285, Oct.–Dec. 2014.

[27] H. Sun, M. Wildemeersch, M. Sheng, and T. Q. S. Quek, "D2D enhanced heterogeneous cellular networks with dynamic TDD," *IEEE Trans. Wireless Commun.*, vol. 14, no. 8, pp. 4204–4218, Aug. 2015.

[28] C. E. Shannon, "A mathematical theory of communication," *Bell Syst. Tech. J.*, vol. 27, no. 3, pp. 379–423, Jul. 1948.

Daisuke Takaishi (S'12) received the B.E. degree in information engineering and the M.S. degree from the Graduate School of Information Science (GSIS), Tohoku University, Sendai, Japan, in 2013 and 2015, respectively. He is currently working toward the Ph.D. degree at the GSIS, Tohoku University. His research interests include UAS networks and ad hoc networks. He was the recipient of the IEEE VTS Japan 2013 Student Paper Award at 78th Vehicular Technology Conference (VTC2013-Fall) and the President's Award of Tohoku University and Dean's Award from Tohoku University.

Yuichi Kawamoto (M'17) received the B.E. degree in information engineering and the M.S. degree and Ph.D. degrees from the Graduate School of Information Science (GSIS), Tohoku University, Sendai, Japan, in 2011, 2013, and 2016, respectively. He is currently an Assistant Professor with the GSIS, Tohoku University, Japan. He was the recipient of the prestigious Deans and Presidents Awards from Tohoku University in March 2016 and several best paper awards at conferences including IWCMC'13, GLOBECOM'13, and WCNC'2014.

Hiroki Nishiyama (SM'13) received the M.S. and Ph.D. degrees in information science from Tohoku University, Sendai, Japan, in 2007 and 2008, respectively. He is currently an Associate Professor with the Graduate School of Information Sciences, Tohoku University, Japan. His research interests include a wide range of areas including satellite communications, unmanned aircraft system (UAS) networks, wireless and mobile networks, ad hoc and sensor networks, green networking, and network security. One of his outstanding achievements is relay-by-smartphone, which makes it possible to share information among many people by using only WiFi functionality of smartphones. He is a senior member of the Institute of Electronics, Information, and Communication Engineers (IEICE). He is an Associate Editor for the IEEE TRANSACTIONS ON VEHICULAR TECHNOLOGY, an Associate Editor for Springer Journal of *Peer-to-Peer Networking and Applications*, and the Secretary for the IEEE ComSoc Sendai Chapter. He has published more than 160 peer-reviewed papers including many high-quality publications in prestigious IEEE journals and conferences. He was the recipient of Best Paper Awards from many international conferences including IEEEs flagship events, such as the IEEE Global Communications Conference in 2014 (GLOBECOM14), GLOBECOM13, and GLOBECOM10, and the IEEE Wireless Communications and Networking Conference in 2014 (WCNC14) and WCNC12. He was also the recipient of the Special Award of the 29th Advanced Technology Award for Creativity in 2015, the IEEE Communications Society Asia–Pacific Board Outstanding Young Researcher Award 2013, the IEICE Communications Society Academic Encouragement Award 2011, and the 2009 FUNAI Foundations Research Incentive Award for Information Technology.

Nei Kato (F'13) received the Bachelor's degree from the Polytechnic University, Tokyo, Japan, in 1986, and the M.S. and Ph.D. degrees in information engineering from Tohoku University, in 1988 and 1991, respectively. He is a Full Professor and the Director of Research Organization of Electrical Communication, Tohoku University, Sendai, Japan. He has been engaged in research on computer networking, wireless mobile communications, satellite communications, ad hoc and sensor and mesh networks, smart grid, IoT, Big Data, and pattern recognition. He has published more than 350 papers in prestigious peer-reviewed journals and conferences. He is a fellow of IEICE. He is the Vice-President-Elect (member and global activities) for the IEEE Communications Society (2018–2019), the Editor-in-Chief for the IEEE Network Magazine (2015–2017), the Editor-in-Chief for the IEEE TRANSACTIONS ON VEHICULAR TECHNOLOGY (2017–present), the Associate Editor-in-Chief for the IEEE INTERNET OF THINGS JOURNAL (2013–present), and the Chair for the IEEE Communications Society Sendai Chapter. He was a Member-at-Large on the Board of a Governors, the IEEE Communications Society (2014–2016), a Vice Chair of Fellow Committee of IEEE Computer Society (2016), a member of the IEEE Computer Society Award Committee (2015–2016) and the IEEE Communications Society Award Committee (2015–2017), the Chair of Satellite and Space Communications Technical Committee (2010–2012) and Ad Hoc and Sensor Networks Technical Committee (2014–2015) of the IEEE Communications Society. He is the recipient of the Minoru Ishida Foundation Research Encouragement Prize (2003), the Distinguished Contributions to Satellite Communications Award from the IEEE Communications Society, Satellite and Space Communications Technical Committee (2005), the FUNAI information Science Award (2007), the TELCOM System Technology Award from Foundation for Electrical Communications Diffusion (2008), the IEICE Network System Research Award (2009), the IEICE Satellite Communications Research Award (2011), the KDDI Foundation Excellent Research Award (2012), the IEICE Communications Society Distinguished Service Award (2012), the IEICE Communications Society Best Paper Award (2012), the Distinguished Contributions to Disaster-Resilient Networks R&D Award from Ministry of Internal Affairs and Communications, Japan (2014), the Outstanding Service and Leadership Recognition Award 2016 from the IEEE Communications Society Ad Hoc and Sensor Networks Technical Committee, the Radio Achievements Award from Ministry of Internal Affairs and Communications, Japan (2016), and the Best Paper Awards from the IEEE ICC/GLOBECOM/WCNC/VTC. He is a Distinguished Lecturer of the IEEE Communications Society and Vehicular Technology Society.

Fumie Ono received the B.E., M.E., and Ph.D. degrees in electrical engineering from Ibaraki University, Mito, Japan, in 1999, 2001, and 2004, respectively. From 2004 to 2006, she was a Research Associate with the Faculty of Engineering, Tokyo University of Science. From 2006 to 2011, she was an Assistant Professor with the Division of Electrical and Computer Engineering, Yokohama National University. She is currently with the Dependable Wireless Lab, Wireless Network Research Institute, National Institute of Information and Communications Technology, Yokosuka, Japan. She is the recipient of the Young Engineer Award from IEICE in 2006 and YRP Award from YRP Award Committee in 2007.

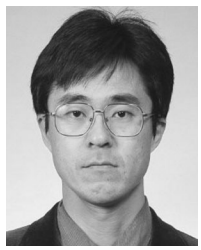

Ryu Miura received the B.E., M.E., and Ph.D. degrees in electrical engineering from Yokohama National University, Yokohama, Japan, in 1982, 1984, and 2000, respectively. In 1984, he joined Radio Research Laboratory, Tokyo, Japan, which was reorganized to National Institute of Information and Communications Technology (NICT), Yokosuka, Japan, in 2004. He is currently an Executive Researcher of Wireless Network Research Center, NICT, where he works on the wireless technologies for unmanned aircraft systems with their application to disaster mitigations and contribution to their safety operations. He is a member of IEICE.